Military Technical College
Kobry El-Kobbah,
Cairo, Egypt.

18th International Conference on Applied Mechanics and Mechanical Engineering.

ANALYSIS OF CUTTING FORCES IN MICRO MILLING

S. Mekhiel*, A. Youssef* and Y. Elshaer*

ABSTRACT

In metal cutting, the prediction of cutting forces has been the focus of research for very long time. The reason for that is to decrease the cost of performing experimental work whenever the cutting of new material is needed. In recent years a new application for metal cutting was introduced due to the miniaturization of components and the invention of micro electro-mechanical system MEMS. This has led to the introduction of micro machining. Thus the analysis of the cutting system needed revisions. This is because of the domination of other factors during cutting process. Among these factors are the minimum chip thickness and the ploughing forces. In this work the modeling of orthogonal, oblique and milling cutting process in micro scale is presented. The results are verified using published experimental results.

KEYWORDS

Cutting forces, micro milling, analytical modeling, face milling and helical end milling.

---

* Egyptian Armed Forces.

INTRODUCTION

The metal cutting process is the process in which metal is removed gradually from the surface of workpiece in the form of chip by shear force. The basic form of cutting process can be described as concentrated shear along certain plane commonly called shear plane[1]. Several models were constructed to describe the force system in orthogonal cutting [2-4]. The slip-stick phenomenon was introduced later to the force model, where there are three different deformation zones as in Fig. 2. Material ahead the tool is basically sheared in area that is called primary shear zone. This chip sticks at, then, it slides with certain sliding friction coefficient. Finally, the flank of the tool rubbing the newly machined surface in the friction area is called tertiary deformation zone as explained by Altintas [5].

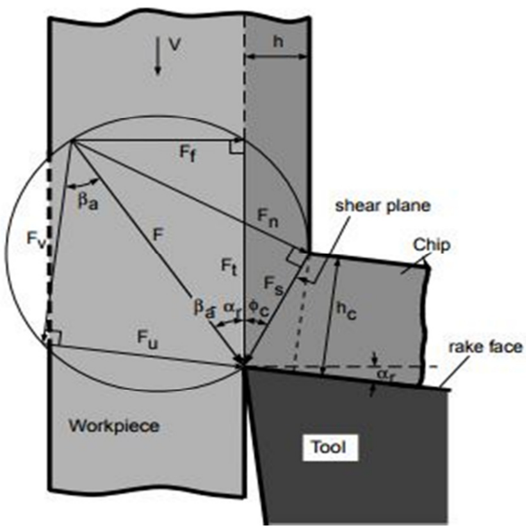

Fig.1. Merchant force model.

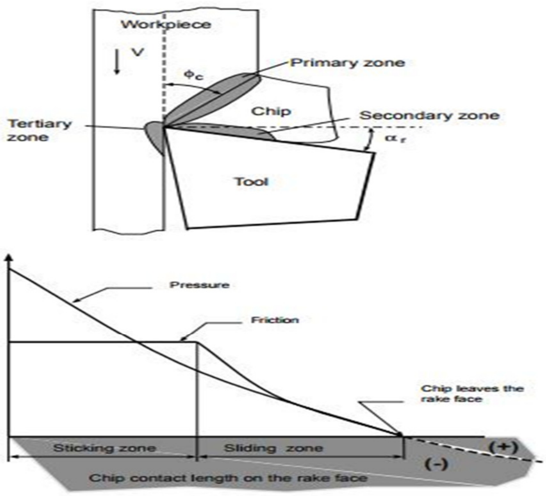

Fig. 2. Three deformation zones and rake face load distribution.

There are two basic different assumptions for analyzing primary shear zone; one of them is assuming the shear zone to be thin plane and that was adopted by Merchant [2], the other, assumes a thick deformation zone as Lee and Shaffer [6] and Palmer and Oxley [7].

PLOUGHING FORCES

Altintas [5, 8] conducted very large number of orthogonal cutting tests for several materials. It was noticed that the measured force components F_t, F_f include two parts; forces due to shearing and forces due to ploughing or rubbing they are called edge forces. This relation can be expressed as:

$$\begin{aligned} F_t &= F_{tc} + F_{te} \\ F_f &= F_{fc} + F_{fe} \end{aligned} \tag{1}$$

The edge force effect is significant during micro scale cutting.

From the geometry in Fig. 1, the tool-chip contact length l_t can be expressed as:

$$l_t = \frac{h \cdot \sin(\phi_c + \beta_a - \alpha_r)}{\sin\phi_c \cdot \cos\beta_a} \tag{2}$$

THEORETICAL PREDICTION OF SHEAR ANGLE

There are two main approaches to predict the shear angle, principle of maximum shear stress and principle of minimum energy.

Maximum shear stress and principle can be explained from the illustrated geometry in Fig. 1, as presented in [5], Krystof, proposed that the angle between shear plane and resultant force equals $(\phi_c + \beta_a - \alpha_r)$. The angle between the principal stress resembled in resultant force direction and maximum shear stress direction should be $\pi/4$. So the relation defining shear angle should be:

$$\phi_c = \frac{\pi}{4} - (\beta_a - \alpha_r) \tag{3}$$

The same relation then was proved using slip-line field theory by Lee and Shaffer[6]. Principle of minimum energy was first used by Merchant[3], as partial derivative of cutting power P_t (which is consisted of cutting velocity V multiplied by tangential or cutting force F_t).

$$\frac{dP_t}{d\phi_c} = \frac{d(V \cdot F_t)}{d\phi_c} \tag{4}$$

It results in $\cos(2 \cdot \phi_c + \beta_a - \alpha_r) = 0$, then

$$\phi_c = \frac{\pi}{4} - \frac{1}{2}(\beta_a - \alpha_r) \tag{5}$$

The exact same formula was proposed previously by Zvorykin [9] but without defining constants A_1 and A_2 as follow:

$$\phi_c = A_1 - A_2(\beta_a - \alpha_r) \tag{6}$$

That form is generalized and more consistent than the other models by changing coefficients A_1 and A_2 as stated in [10].However, the previously mentioned formulae are not accurate due to over simplification in assumptions. But they clarify the dependency of ϕ_c on both α_r and β_a and the significance of these two parameters.

FORMULATION OF FORCES SYSTEM IN MILLING

In milling operations, the uncut chip thickness is completely different than turning because it is variable. It can be introduced as function of instantaneous immersion angle ϕ. Knowing the value of feed rate per tooth c, then approximately

$$h(\phi) = c \sin \phi \tag{7}$$

For simplicity the helix angle β is considered to be zero as in face milling operations with inserts. Butting value for edge contact length a then milling cutting forces can be expressed as follow;

$$\begin{aligned} F_t(\phi) &= K_{tc} \cdot a \cdot h(\phi) + K_{te} \cdot a \\ F_r(\phi) &= K_{rc} \cdot a \cdot h(\phi) + K_{re} \cdot a \\ F_a(\phi) &= K_{ac} \cdot a \cdot h(\phi) + K_{ae} \cdot a \end{aligned} \tag{8}$$

As K_{te}, K_{re}, and K_{ae} are edge constants in tangential, radial, and axial directions respectively, also K_{tc}, K_{rc}, and K_{ac} are cutting coefficients due to contribution of shearing. In equations (8) it can be noticed that each force component consists of two different parts; first one is from cutting or shearing, while the other is from ploughing. These ploughing forces are the same as edge forces same mentioned in(1). Axial component of force F_a can be ignored for infinitely sharp cutting edge (with nose radius $r = 0$)[5].

The cutting coefficients are assumed to be constant for the same material pair of tool and workpiece, they could be obtained from analogy of oblique cutting forces, or mechanistically obtained using series of experimental tests from which coefficients can be calibrated directly. The latter mechanistic method could be used to get also edge coefficients. The former relations are linear, Rodriguez [11] modeled milling operation with that form, despite being not so realistic and ignoring a lot of significant parameters like speed dependency for some materials or size effect due to nose radius variation.

Speed dependency is the variation of material behavior like differences in yield strength or coefficient of friction with the change of cutting speed, this form of non-linearity cannot be detected with the linear formula coefficients, so other nonlinear formulas are used. Jin[12] and [13] concluded that the nonlinearity was due to usual uncut chip thickness variation along with nose radius variations.

Finally from forces equilibrium diagram for the cutting forces along with the cutter geometry the following equations can be derived,

$$F_x(\phi) = -F_t \cdot \cos\phi - F_r \cdot \sin\phi$$
$$F_y(\phi) = F_t \cdot \sin\phi - F_r \cdot \cos\phi \quad (9)$$
$$F_z(\phi) = F_a$$

MECHANISTIC PREDICTION OF CUTTING FORCES

Among the different modeling techniques mechanistic modeling is the most commonly used technique for cutting force prediction [12, 14, 15]. It is considered semi empirical modeling technique as it joins both advantages of analytical and empirical models. Mechanistic modeling depends mainly on the relation between cutting force coefficients and force value as presented in Eqns. (10) and(11);

$$F_t = b \cdot h \cdot \left(\frac{\tau_s \cdot \cos(\beta_a - \alpha_r)}{\sin\phi_c \cdot \cos(\phi_c + \beta_a - \alpha_r)} \right)$$
$$F_f = b \cdot h \cdot \left(\frac{\tau_s \cdot \sin(\beta_a - \alpha_r)}{\sin\phi_c \cdot \cos(\phi_c + \beta_a - \alpha_r)} \right) \quad (10)$$

$$K_t = \frac{\tau_s \cdot \cos(\beta_a - \alpha_r)}{\sin\phi_c \cdot \cos(\phi_c + \beta_a - \alpha_r)}$$
$$K_f = \frac{\tau_s \cdot \sin(\beta_a - \alpha_r)}{\sin\phi_c \cdot \cos(\phi_c + \beta_a - \alpha_r)} \quad (11)$$

Force prediction is generalized as:

$$F_{t,r,a} = K_{(t,r,a)c} \cdot b \cdot h + K_{(t,r,a)e} \quad (12)$$

With (t, r, a) (tangential, radial, and axial), this technique can deal with very complicated tool geometries by integrating the mentioned force coefficients along the entire tool surface. This model it needs to be calibrated by cutting tests. However, Armarego [16] unified model can be used to get cutting constants. The uncertainty of this technique after that calibration is less than 5% as stated by Arrazola et al. [17]. This can be modeled commonly by FEM as replacement for expensive cutting tests as in [12, 13].

MATHEMATICAL FORMULATION

Orthogonal Cutting Analysis

From orthogonal cutting geometry in merchant approach, the force relations are as follow,

$$F = \sqrt{F_f^{\,2} + F_t^2}$$
$$F_t = F \cdot \cos(\beta_a - \alpha_r) \quad (13)$$
$$F_r = F \cdot \sin(\beta_a - \alpha_r)$$

Shear and normal forces can be derived from the geometry as follow:

$$F_s = F\cos(\phi_c + \beta_a - \alpha_r)$$
$$F_n = F\sin(\phi_c + \beta_a - \alpha_r) \quad (14)$$

where ϕ_c is shear angle, α_r is tool rake angle, and β_a is average friction angle between moving chip and rake face of the tool. They also can be expressed as function of feed and tangential forces as:

$$F_s = F_t\cos\phi_c - F_f\sin\phi_c$$
$$F_n = F_t\sin\phi_c + F_f\cos\phi_c \quad (15)$$

Using same transformation on the secondary shear or deformation zone frictional force and normal friction force can be written also in terms of α_r, F_t and F_f as follow:

$$F_v = F_t\cos\alpha_r - F_f\sin\alpha_r$$
$$F_u = F_t\sin\alpha_r + F_f\cos\alpha_r \quad (16)$$

From the relation between F_v and F_u the values of friction angle β_a and the average frictional coefficient μ_a are obtained as given in [18]:

$$F_u = F\cdot\sin\beta_a$$
$$F_v = F\cdot\cos\beta_a \quad (17)$$

$$\mu_a = \tan\beta_a = \frac{F_u}{F_v} \quad (18)$$

Merging (18) with (16)

$$\beta_a = \tan^{-1}\left(\frac{F_t\cos\alpha_r - F_f\sin\alpha_r}{F_t\sin\alpha_r + F_f\cos\alpha_r}\right) \quad (19)$$

Using only geometry shear angle can be derived as

$$\phi_c = \tan^{-1}\frac{r_c\cdot\cos\alpha_r}{1 - r_c\cdot\sin\alpha_r} \quad (20)$$

Another value could be predicted is the value of shear stress τ_s, it is defined as shear force F_s over shear plane area $A_s = b\cdot h/\sin\phi_c$ knowing that b is value of width of cut or depth of cut in turning.

$$\tau_s = \frac{F_s}{A_s} \quad (21)$$

From(21) and(15)

$$\tau_s = \frac{\left(F_t\cos\phi_c - F_f\sin\phi_c\right)\cdot\sin\phi_c}{b\cdot h} \quad (22)$$

Oblique Cutting Model

The main difference between orthogonal and normal cutting is the inclination angle or oblique angle (i). This leads to the existence of new components for shear direction, friction, and chip flow. Normal shear angle ϕ_n is the angle enclosed between shear direction and xy plane, and oblique shear angle ϕ_i is the angle enclosed between shear direction and xz plane. Another angle η is introduced as the chip flow angle between chip flow direction and direction normal to cutting edge on the rake face plane, that direction normal to cutting edge on the rake face is inclined to z axis with angle α_n which is called normal rake angle.

Determination of oblique cutting parameters

Beginning with relation defining η chip flow angle in terms of normal rake, oblique, and normal shear angles[1].

$$\tan\eta = \frac{\tan i \cdot \cos(\phi_n - \alpha_n) - \cos\alpha_n \cdot \tan\phi_i}{\sin\phi_n} \tag{23}$$

From the geometry in Fig.3**Error! Reference source not found.** and definition of friction angle in (17) the resultant force angles relations can be deduced as follows:

$$\begin{aligned} \sin\theta_i &= \sin\beta_a \cdot \sin\eta \\ \tan(\theta_n + \phi_n) &= \tan\beta_a \cdot \cos\eta \end{aligned} \tag{24}$$

Using the maximum shear stress approach will lead to:

$$\begin{aligned} \sin\phi_i &= \sqrt{2} \cdot \sin\theta_i \\ \cos(\phi_n + \theta_n) &= \frac{\tan\theta_i}{\tan\phi_i} \end{aligned} \tag{25}$$

Using Minimum energy approach will lead to:

$$\begin{aligned} \frac{\partial P_t`}{\partial\phi_n} &= 0 \\ \frac{\partial P_t`}{\partial\phi_i} &= 0 \end{aligned} \tag{26}$$

Knowing that the value of $P_t`$ can be defined from geometry and forces relations as:

$$\begin{aligned} P_t` &= \frac{P_t}{V \cdot b \cdot h \cdot \tau_s} \\ P_t` &= \frac{\cos\theta_n + \tan\theta_i \cdot \tan i}{\sin\phi_n \cdot \left(\cos(\phi_n + \theta_n) \cdot \cos\phi_i + \tan\theta_i \cdot \sin\phi_i\right)} \end{aligned} \tag{27}$$

The model has five different unknown parameters $(\phi_n, \phi_i, \theta_n, \theta_i, \eta)$ to solve these parameters that implies iterative procedure with initial assumption of Stabler rule ($i = \eta$)[19].

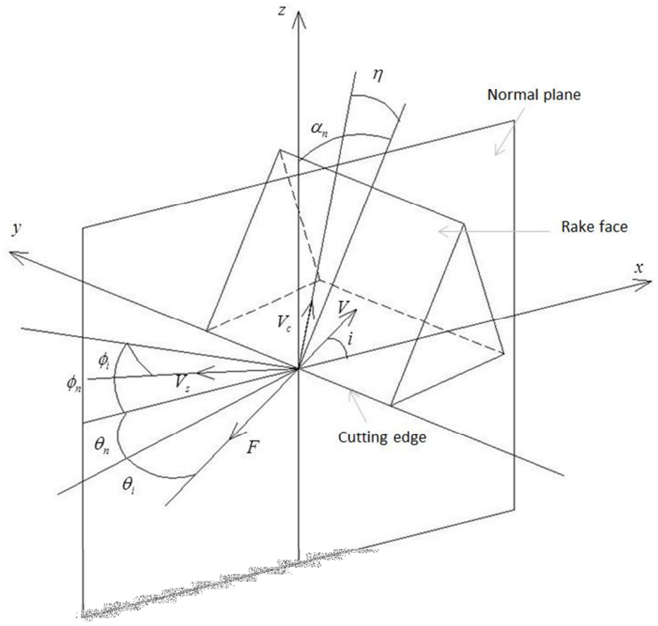

Fig.3. Oblique cutting geometry.

However there is another approach proposed by Armarego[16] based on Stabler assumptions[19]; both shear force and velocity have the same direction and chip length ratio remain with the same value as in orthogonal cutting, introducing normal friction angle (β_n)

$$\tan\beta_n = \tan\beta_a \cdot \cos\eta \tag{28}$$

Combining previous geometry equations we get:

$$\tan(\phi_n + \beta_n) = \frac{\cos\phi_n \cdot \tan i}{\tan\eta - \sin\phi_n \cdot \tan i} \tag{29}$$

Finally from experiments conducted by Armarego[16] the following formula for normal shear angle was proposed.

$$\tan\phi_c = \frac{r_c \cdot \left(\cos\eta / \cos i \right) \cdot \cos\alpha_r}{1 - r_c \cdot \left(\cos\eta / \cos i \right) \cdot \sin\alpha_r} \tag{30}$$

Solving the last three equations numerically we get ϕ_n, β_n, η or apply former Stabler rule ($i = \eta$)[19] and get them directly.

Cutting forces prediction

In oblique cutting, the resultant force is as follows:

$$F = \frac{b \cdot h \cdot \tau_s}{\sin\phi_n \cdot \cos i \cdot \left(\cos(\phi_n + \theta_n) \cdot \cos\phi_i \cdot \cos\theta_i + \sin\theta_i \cdot \sin\phi_i \right)} \tag{31}$$

From geometry;

$$F_t = \frac{b \cdot h \cdot \tau_s \cdot \left(\cos\theta_n + \tan\theta_i \cdot \tan i\right)}{\sin\phi_n \left(\cos\left(\phi_n + \theta_n\right) \cdot \cos\phi_i + \tan\theta_i \cdot \sin\phi_i\right)}$$
$$F_f = \frac{b \cdot h \cdot \tau_s \cdot sin\theta_n}{\sin\phi_n \cdot \cos i \cdot \left(\cos\left(\phi_n + \theta_n\right) \cdot \cos\phi_i + \tan\theta_i \cdot \sin\phi_i\right)} \quad (32)$$
$$F_r = \frac{b \cdot h \cdot \tau_s \cdot \left(\tan\theta_i - \cos\theta_n \cdot \tan i\right)}{\sin\phi_n \left(\cos\left(\phi_n + \theta_n\right) \cdot \cos\phi_i + \tan\theta_i \cdot \sin\phi_i\right)}$$

Forces can be expressed in the following form:

$$F_t = K_{tc} \cdot b \cdot h + K_{te} \cdot b$$
$$F_f = K_{fc} \cdot b \cdot h + K_{fe} \cdot b \quad (33)$$
$$F_r = K_{rc} \cdot b \cdot h + K_{re} \cdot b$$

Then,

$$K_{tc} = \frac{\tau_s \cdot \left(\cos\theta_n + \tan\theta_i \cdot \tan i\right)}{\sin\phi_n \left(\cos\left(\phi_n + \theta_n\right) \cdot \cos\phi_i + \tan\theta_i \cdot \sin\phi_i\right)}$$
$$K_{fc} = \frac{\tau_s \cdot sin\theta_n}{\sin\phi_n \cdot \cos i \cdot \left(\cos\left(\phi_n + \theta_n\right) \cdot \cos\phi_i + \tan\theta_i \cdot \sin\phi_i\right)} \quad (34)$$
$$K_{rc} = \frac{\tau_s \cdot \left(\tan\theta_i - \cos\theta_n \cdot \tan i\right)}{\sin\phi_n \left(\cos\left(\phi_n + \theta_n\right) \cdot \cos\phi_i + \tan\theta_i \cdot \sin\phi_i\right)}$$

According to geometrical relations of classical oblique model cutting force components can be introduced as:

$$F_t = b \cdot h \cdot \left(\frac{\tau_s}{\sin\phi_n} \cdot \frac{\cos\left(\beta_n - \alpha_n\right) + \tan i \cdot \tan\eta \cdot \sin\beta_n}{\sqrt{\cos^2\left(\phi_n + \beta_n - \alpha_n\right) + \tan^2\eta \cdot \tan^2\beta_n}} \right)$$
$$F_f = b \cdot h \cdot \left(\frac{\tau_s}{\sin\phi_n \cdot \cos i} \cdot \frac{\sin\left(\beta_n - \alpha_n\right)}{\sqrt{\cos^2\left(\phi_n + \beta_n - \alpha_n\right) + \tan^2\eta \cdot \tan^2\beta_n}} \right) \quad (35)$$
$$F_r = b \cdot h \cdot \left(\frac{\tau_s}{\sin\phi_n} \cdot \frac{\cos\left(\beta_n - \alpha_n\right) \cdot \tan i - \tan\eta \cdot \sin\beta_n}{\sqrt{\cos^2\left(\phi_n + \beta_n - \alpha_n\right) + \tan^2\eta \cdot \tan^2\beta_n}} \right)$$

Then

$$K_{tc} = \frac{\tau_s}{\sin\phi_n} \cdot \frac{\cos\left(\beta_n - \alpha_n\right) + \tan i \cdot \tan\eta \cdot \sin\beta_n}{\sqrt{\cos^2\left(\phi_n + \beta_n - \alpha_n\right) + \tan^2\eta \cdot \tan^2\beta_n}}$$
$$K_{fc} = \frac{\tau_s}{\sin\phi_n \cdot \cos i} \cdot \frac{\sin\left(\beta_n - \alpha_n\right)}{\sqrt{\cos^2\left(\phi_n + \beta_n - \alpha_n\right) + \tan^2\eta \cdot \tan^2\beta_n}} \quad (36)$$
$$K_{rc} = \frac{\tau_s}{\sin\phi_n} \cdot \frac{\cos\left(\beta_n - \alpha_n\right) \cdot \tan i - \tan\eta \cdot \sin\beta_n}{\sqrt{\cos^2\left(\phi_n + \beta_n - \alpha_n\right) + \tan^2\eta \cdot \tan^2\beta_n}}$$

Using Altintas[8], assumptions to join orthogonal tests with the unified model in(36). These assumptions are ($\alpha_n \equiv \alpha_r$) normal rake angle equals orthogonal cutting rake angle, $(\phi_c \equiv \phi_n)$ normal shear angle also equals orthogonal cutting shear angle, shear stress τ_s and average friction angle β_a are the same in both orthogonal and oblique cutting, and $(\eta \equiv i)$ the oblique angle equals chip flow angle adopting Stabler rule[19].

Milling Process Models

Milling process can be first treated as face milling process then it can be generalized in more complex form of end milling considering larger values of depth of cut and effect of the helix angle.

Face milling model

The face milling model in Fig. 4 is general case for face milling where ϕ_{st} and ϕ_{ex} both have values not equal to zero, and immersion angle ϕ is measured for certain cutting edge. The hatched area is the instantaneous shape of chip load or uncut chip thickness per tooth. Circular path is shown where h can be expressed as function of ϕ as follows:

$$h(\phi) = c \cdot \sin\phi \tag{37}$$

h is the instantaneous value of chip load for certain cutting edge/flute, c is the feed per revolution or tooth ,and ϕ is the immersion angle.

Average chip load per revolution can be calculated from the hatched zone as follows:

$$h_a = \frac{\int_{\phi_{st}}^{\phi_{ex}} c \cdot \sin\phi \cdot d\phi}{\phi_{ex} - \phi_{st}} = \frac{-c\left(\cos\phi_{ex} - \cos\phi_{st}\right)}{\phi_{ex} - \phi_{st}} \tag{38}$$

Force components can be expressed in terms of varying chip load $h(\phi)$ and axial depth of cut or edge contact length a, as follows:

$$\begin{aligned} F_t(\phi) &= \left(K_{tc} \cdot h(\phi) + K_{te}\right) \cdot a \\ F_r(\phi) &= \left(K_{rc} \cdot h(\phi) + K_{re}\right) \cdot a \\ F_a(\phi) &= \left(K_{ac} \cdot h(\phi) + K_{ae}\right) \cdot a \end{aligned} \tag{39}$$

Using Cartesian forces from (9), and knowing that all force components have values if and only if $\phi_{st} \le \phi \le \phi_{ex}$, or when $h(\phi)$ has non-zero value.

Milling operation of course is a multi-edge operation, so for the single tool has one or more flutes, then the angle between these flutes is called cutter pitch angle or tooth spacing angle ϕ_p, N_f is the number of flutes or cutting edges, then cutter pitch angle in radians equals to:

$$\phi_p = \frac{2 \cdot \pi}{N_f}. \tag{40}$$

A mathematical model for predicting the cutting forces during face milling was constructed on MATLAB.R2013a®. This model`s results were compared to Altintas [5] results in three different cases; up milling and down milling half immersion then,

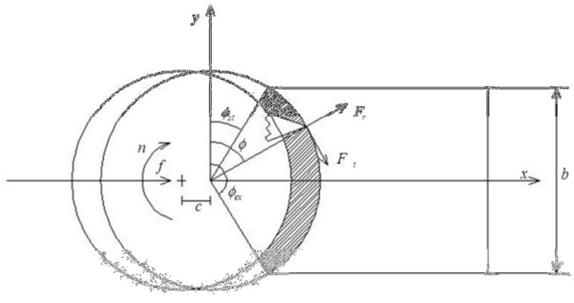

Fig. 4. Variable chip load and immersion angles in milling.

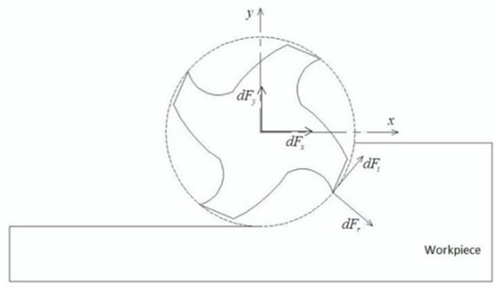

Fig. 5. Differential force components in down milling case.

center face milling from 75 to 105 degree start and exit immersion angles respectively.

The model could predict all cutting force components for face milling operations once K_t, K_r had been obtained mechanistically. Simplified flowchart for presented model is demonstrated in Fig. **6**.

End milling model

End milling operations is modeled by expanding the derived force model by increasing axial depth of cut and helix angle end milling model can be constructed. The tool is divided into differential parts "disks" in z direction as shown in Fig. 7 and consider every part behavior the same as face milling with only tangential and radial components

To model end milling the lag angle is defined β as follows:

$$\psi = \frac{2 \cdot z \cdot \tan \beta}{D} \quad (41)$$

Another mathematical model for prediction of cutting force components in case of end milling was also created using MATLAB.R2013a®. Its results were compared to results of [8, 20] and good agreement was found. The normal shear angle is then,

$$\phi_n = \tan^{-1} \frac{r_c \cdot \cos \alpha_r}{1 - r_c \cdot \sin \alpha_r} \quad (42)$$

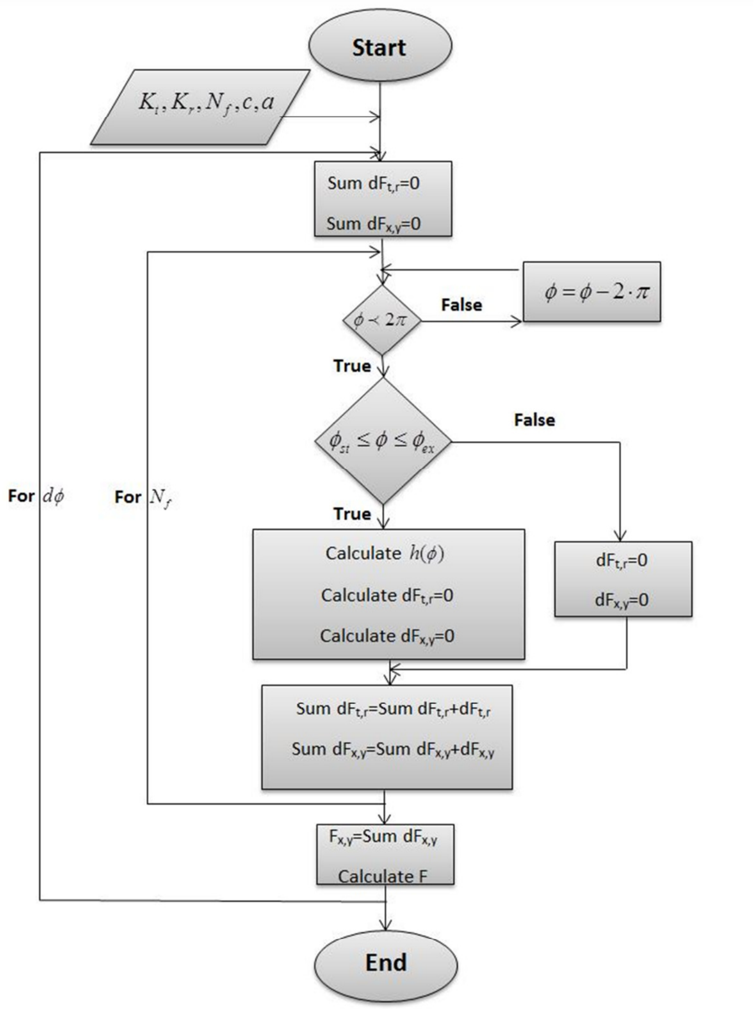

Fig. 6. Flowchart for face milling code.

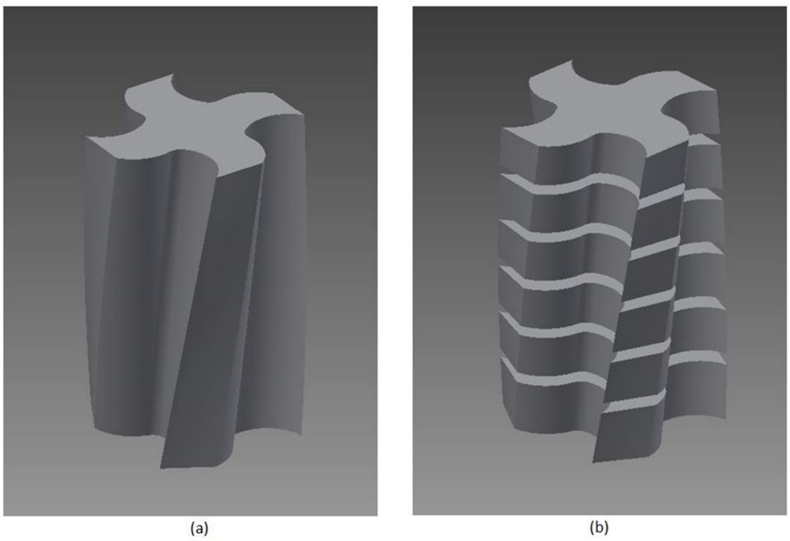

Fig. 7. Simulated end mill with 4 flutes (a) Normal (b) Discretized**.**

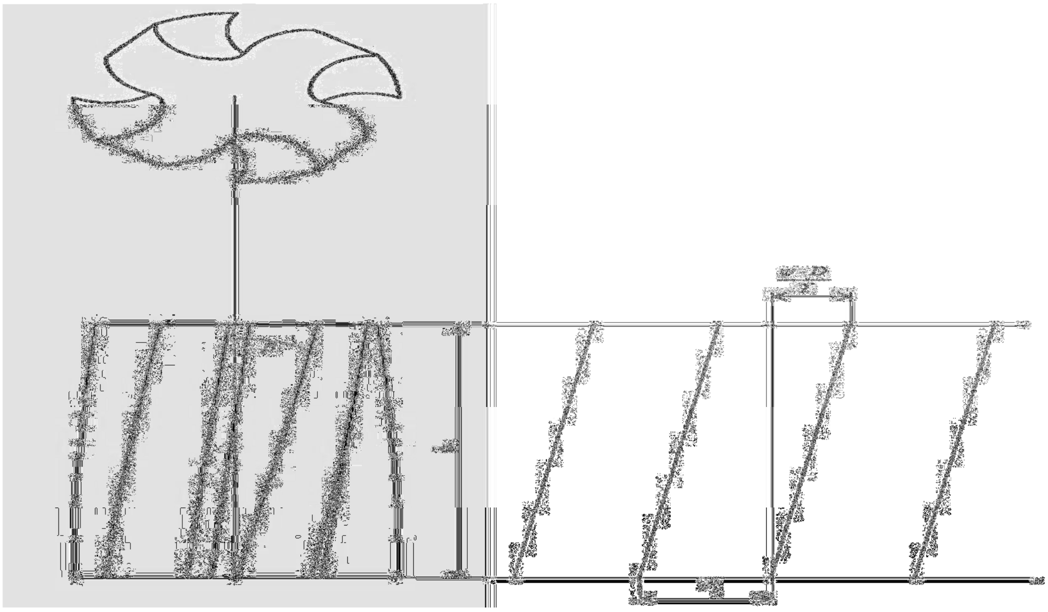

Fig. 8. Lag angle for z=a.

and $i \equiv \eta$ from Stabler rule for chip flow [19], also understanding the geometry of milling operation the oblique angle in oblique cutting has the same definition as helix angle in milling $(i = \beta)$, (36) can be represented as follows:

$$K_{tc} = \frac{\tau_s}{\sin\phi_n} \cdot \frac{\cos(\beta_a - \alpha_r) + \tan\beta \cdot \tan\beta \cdot \sin\beta_a}{\sqrt{\cos^2(\phi_n + \beta_a - \alpha_r) + \tan^2\beta \cdot \tan^2\beta_a}}$$
$$K_{fc} = \frac{\tau_s}{\sin\phi_n \cdot \cos\beta} \cdot \frac{\sin(\beta_a - \alpha_r)}{\sqrt{\cos^2(\phi_n + \beta_a - \alpha_r) + \tan^2\beta \cdot \tan^2\beta_a}} \quad (43)$$
$$K_{rc} = \frac{\tau_s}{\sin\phi_n} \cdot \frac{\cos(\beta_a - \alpha_r) \cdot \tan\beta - \tan\beta \cdot \sin\beta_a}{\sqrt{\cos^2(\phi_n + \beta_a - \alpha_r) + \tan^2\beta \cdot \tan^2\beta_a}}$$

Now from tool geometry β, α_r are known and ϕ_n can be calculated from Eqn. (42), with the required material orthogonal cutting database.

Mechanistic Model Formulation

Instead of time consuming construction of database from orthogonal cutting then deriving oblique cutting constants, there is practical method that can be used to determine milling constants. Simply conduct set of experiments conserving the same axial depth of cut and immersion usually full immersion for simplification. Then to avoid the effect of tool run out the total force components on the spindle are measured then divided by flutes number. Average force per tooth $\overline{F_q}$ is obtained from start immersion angle to exit immersion angle ($q = x, y, z$) as:

$$\overline{F_q} = \int_{\phi_{st}}^{\phi_{ex}} \frac{F_q(\phi)}{\phi_p} d\phi \quad (44)$$

Integrating the instantaneous force components then applying $\phi_{st} = 0$ and $\phi_{ex} = \pi$ which are the typical full immersion case conditions, then we get:

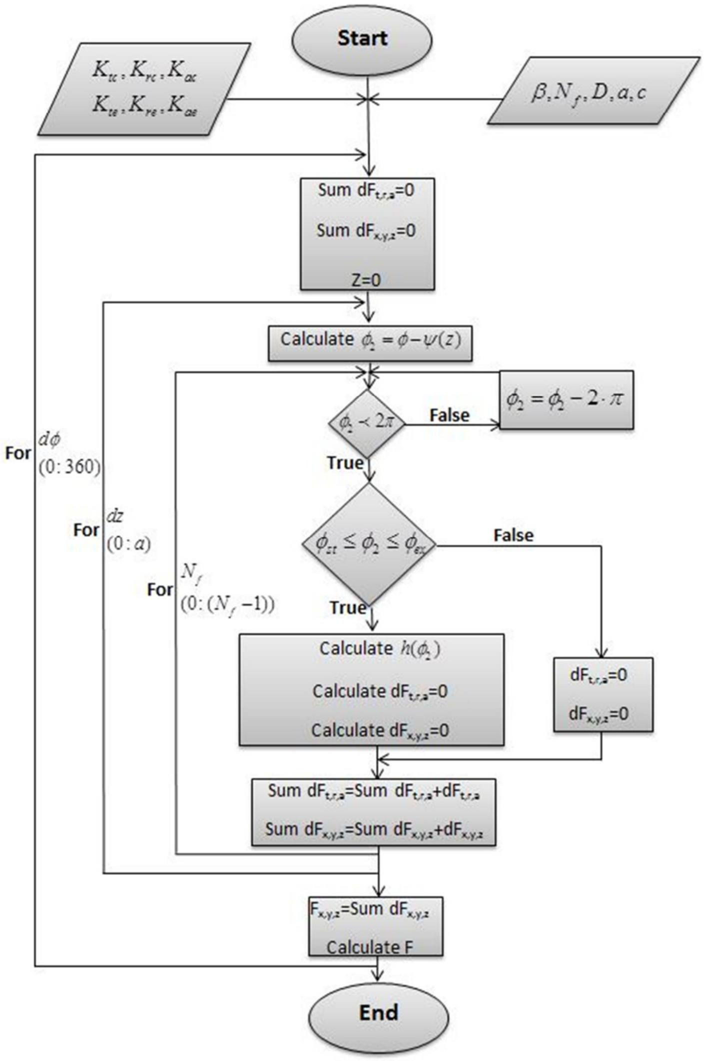

Fig. 9. Flowchart for helical end milling code.

$$\begin{aligned}
\overline{F_x} &= -\frac{N_f \cdot a}{4} \cdot K_{rc} \cdot c - \frac{N_f \cdot a}{\pi} \cdot K_{re} \\
\overline{F_y} &= \frac{N_f \cdot a}{4} \cdot K_{tc} \cdot c + \frac{N_f \cdot a}{\pi} \cdot K_{te} \\
\overline{F_z} &= \frac{N_f \cdot a}{\pi} \cdot K_{ac} \cdot c + \frac{N_f \cdot a}{2} \cdot K_{ae}
\end{aligned} \tag{45}$$

Introducing linear function of feed and edge and cutting components as:

$$\overline{F_q} = \overline{F_{qc}} \cdot c + \overline{F_{qe}} \tag{46}$$

Then

$$\begin{aligned}
K_{tc} &= \frac{4 \cdot \overline{F_{yc}}}{N_f \cdot a}, K_{rc} = \frac{-4 \cdot \overline{F_{xc}}}{N_f \cdot a}, K_{ac} = \frac{\pi \cdot \overline{F_{zc}}}{N_f \cdot a} \\
K_{te} &= \frac{\pi \cdot \overline{F_{ye}}}{N_f \cdot a}, K_{re} = \frac{-\pi \cdot \overline{F_{xe}}}{N_f \cdot a}, K_{ae} = \frac{2 \cdot \overline{F_{ze}}}{N_f \cdot a}
\end{aligned} \tag{47}$$

RESULTS AND DISCUSSION

Face milling force prediction model was constructed using MATLAB,. Some results are shown in the following figures, and they are as follow; half immersion up milling with angles ($\phi_{st} = 0^\circ, \phi_{ex} = 90^\circ$) in Fig.10. The resultant force is increasing periodically until the angle reach $\phi = 90^\circ$ where the cutting tooth became out of cut then the resultant force value fall to zero then rise again as the tool pitch angle is equal to immersion angle.

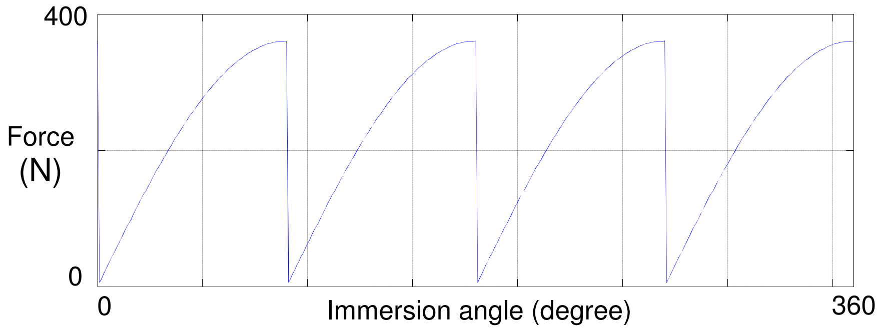

Fig.10. Half immersion up face milling with 4 flutes cutter.

Half immersion down milling with angles ($\phi_{st} = 90^\circ, \phi_{ex} = 180^\circ$) is presented in Fig.11. The resultant force is decreasing periodically until the angle reach $\phi = 90^\circ$ the resultant force reaches its lower value as the cutting tooth became out of cut then it rises again as the undeformed chip thickness arises in front of the following tooth, then the same behavior is repeated.

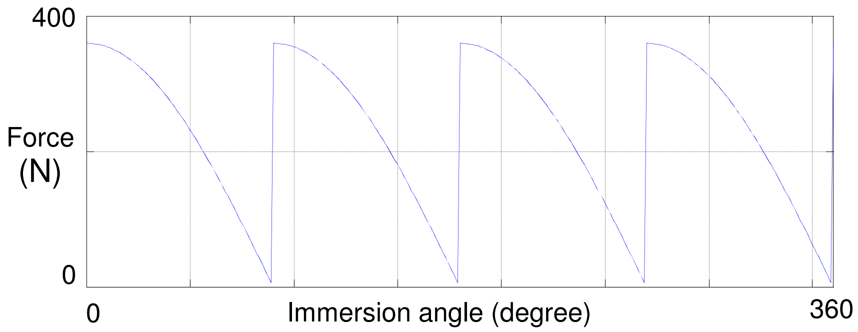

Fig.11. Half immersion down face milling with 4 flutes cutter.

Center face milling simulation with angles ($\phi_{st} = 75^\circ, \phi_{ex} = 105^\circ$) as general case for face milling is illustrated in Fig.12 The force only occurs in the period in which any of cutting flutes is engaged.

All these predictions are for cutter with four flutes, edge contact length $2mm$, feed rate per tooth $0.1mm / tooth$, $K_t = 1800MPa$, and $K_r = 0.3$. These results are in a good agreement with work reported by Altintas [5]. The previous cases did not include any overlaps between two flutes simultaneously. The presented model is applied on full immersion case for the same cutter with four flutes. The result is shown in Fig.13.

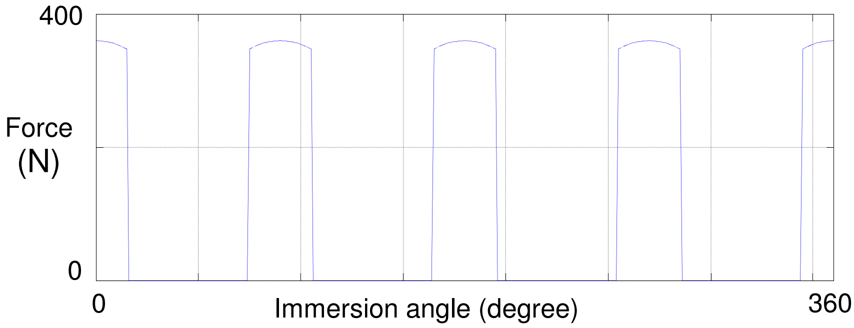

Fig.12. Center face milling with 4 flutes cutter 75:105.

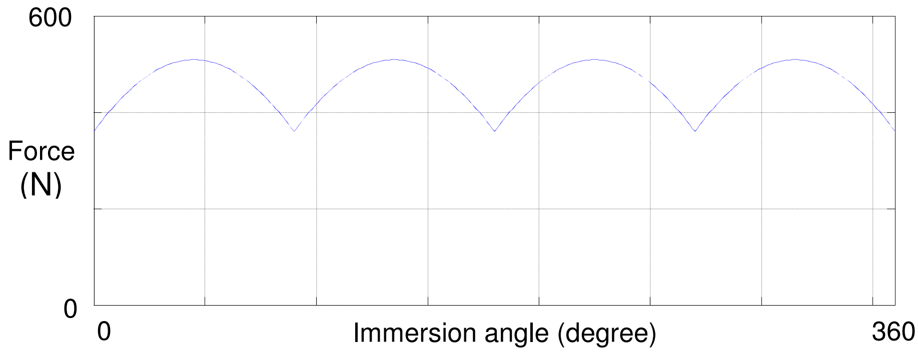

Fig.13. Full immersion with 4 flutes cutter.

The used tool in the presented work has six flutes. So the model is applied for up milling and down milling in half immersion case in Fig.14 and Fig.15, respectively.

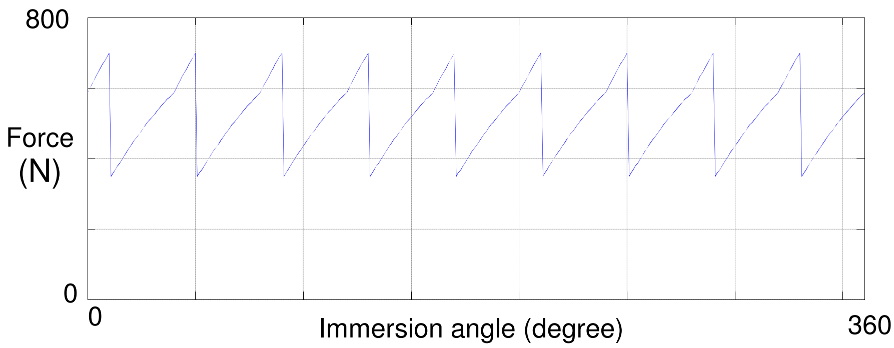

Fig.14. Half immersion up face milling with 6 flutes cutter.

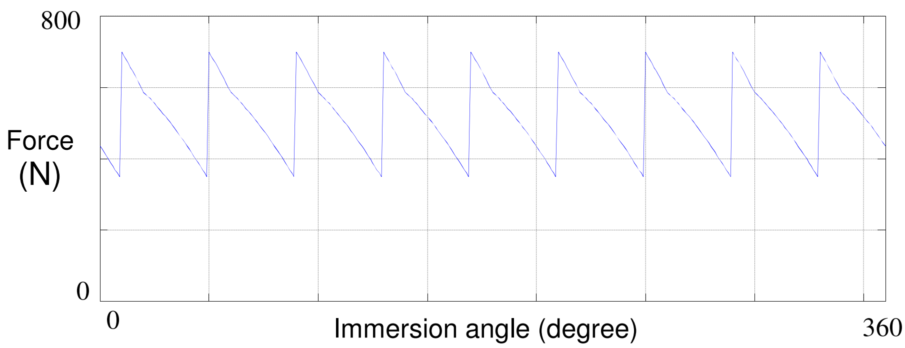

Fig.15. Half immersion down face milling with 6 flutes cutter.

The face milling model is generalized to model the helical end milling process and evaluate its cutting forces. The model results show matching behavior to the published work of Altintas[8]. These results are shown in Fig.16.

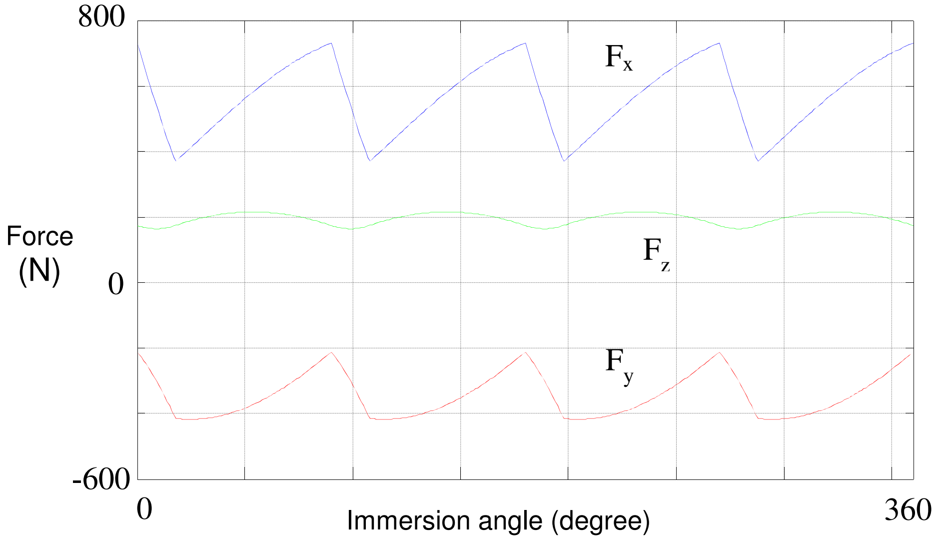

Fig.16. Force components in helical end milling.

CONCLUSION

The modeling of cutting forces in micro scale milling was presented. Normal, oblique force analysis was explained. Face milling force prediction code was created and evaluated demonstrating the behavior of forces in different cases. Summation of force was added to the code to generalize the use of it. The ploughing force effect was demonstrated and used in models. Also model for helical end milling was constructed and evaluated as well. It was shown that this force system is different from the ordinary macro scale. The results from the constructed models were then compered to work found in literature. The results were in agreement with experimental work previously published.

REFERENCES

[1] M. E. Merchant, "Basic mechanics of the metal-cutting process", *ASME J. of Applied Mechanics,* vol. 11, p. A168, 1944.

[2] M. E. Merchant, "Mechanics of the metal cutting process. I. Orthogonal cutting and a type 2 chip", *Journal of applied physics,* vol. 16, pp. 267-275, 1945.

[3] M. E. Merchant, "Mechanics of the metal cutting process. II. Plasticity conditions in orthogonal cutting", *Journal of applied physics,* vol. 16, pp. 318-324, 1945.

[4] M. C. Shaw and J. Cookson, *Metal cutting principles* vol. 2: Oxford university press New York, 2005.

[5] Y. Altintas, *Manufacturing automation: metal cutting mechanics, machine tool vibrations, and CNC design*: Cambridge university press, 2000.

[6] E. Lee and B. Shaffer, "The theory of plasticity applied to a problem of machining", *Journal of applied mechanics,* vol. 18, pp. 405-413, 1951.

[7] W. Palmer and P. Oxley, "Mechanics of orthogonal machining", *Proceedings of the Institution of Mechanical Engineers,* vol. 173, pp. 623-654, 1959.
[8] Y. Altinta and E. Armarego, "Prediction of milling force coefficients from orthogonal cutting data", *Trans. ASME J. Engng Ind,* 1996.
[9] K. Zvorykin, "Work and stress necessary for separation of metal chips", *Proceedings of the Kharkov Technological Institute, Ukraine,* 1893.
[10] D. Germain, G. Fromentin, G. Poulachon, and S. Bissey-Breton, "From large-scale to micromachining: A review of force prediction models", *Journapl of Manufacturing Processes,* vol. 15, pp. 389-401, 2013.
[11] P. Rodríguez and J. Labarga, "A new model for the prediction of cutting forces in micro-end-milling operations", *Journal of Materials Processing Technology,* vol. 213, pp. 261-268, 2013.
[12] X. Jin and Y. Altintas, "Prediction of micro-milling forces with finite element method", *Journal of Materials Processing Technology,* vol. 212, pp. 542-552, 2012.
[13] S. Afazov, S. Ratchev, and J. Segal, "Modelling and simulation of micro-milling cutting forces", *Journal of Materials Processing Technology,* vol. 210, pp. 2154-2162, 2010.
[14] S. Park and M. Malekian, "Mechanistic modeling and accurate measurement of micro end milling forces," *CIRP Annals-Manufacturing Technology,* vol. 58, pp. 49-52, 2009.
[15] Y. Srinivasa and M. Shunmugam, "Mechanistic model for prediction of cutting forces in micro end-milling and experimental comparison", *International Journal of Machine Tools and Manufacture,* vol. 67, pp. 18-27, 2013.
[16] E. Armarego and R. Whitfield, "Computer based modelling of popular machining operations for force and power prediction", *CIRP Annals-Manufacturing Technology,* vol. 34, pp. 65-69, 1985.
[17] P. Arrazola, T. Özel, D. Umbrello, M. Davies, and I. Jawahir, "Recent advances in modelling of metal machining processes", *CIRP Annals-Manufacturing Technology,* vol. 62, pp. 695-718, 2013.
[18] N. Zorev, "Inter-relationship between shear processes occurring along tool face and shear plane in metal cutting", *International research in production engineering,* vol. 49, pp. 42-49, 1963.
[19] G. Stabler, "The chip flow law and its consequences", *Advances in Machine Tool Design and Research,* vol. 5, pp. 243-251, 1964.
[20] Y. Altintaş and P. Lee, "A general mechanics and dynamics model for helical end mills", *CIRP Annals-Manufacturing Technology,* vol. 45, pp. 59-64, 1996.